

Extraction of α_s using data from H1

DESY Summer Student Program 2010

Mohamed Sadok ZIDI

Jijel University, Algeria
zidisadok@yahoo.com

Supervisors: Dr. G. Grindhammer, D. Britzger

H1 Group, MPI Munich
guenterg@desy.de, daniel.britzger@desy.de

Abstract

This report gives a summary of my DESY summer school 2010 project, during my work with MPI Munich group of the H1 collaboration.

We studied the fit of the strong coupling constant using inclusive jet production in neutral current deep-inelastic positron-proton scattering at large four momentum transfer squared $Q^2 > 150\text{GeV}^2$ with the H1 detector at HERA. The running of the strong coupling is demonstrated and the value of $\alpha_s(M_z)$ is determined to $\alpha_s(M_z) = 0.11781 \pm 0.00232$.

Contents

1	Introduction	3
1.1	HERA accelerator	3
1.2	DIS process at HERA	3
1.3	Jet production in Deep-Inelastic Scattering	4
2	Cross section calculation	5
2.1	NLO jet cross section	5
2.2	fastNLO	6
	2.2.1 fastNLO principle	6
	2.2.2 FastNLO Calculation	7
3	Fitting techniques	7
3.1	χ^2 definition	8
3.2	Source of errors	8
3.3	Minimization of χ^2 using Minuit	9
4	α_s extraction	9

1 Introduction

1.1 HERA accelerator

The HERA collider (for Hadron Electron Ring Anlage) is an electron-proton collider at DESY, Hamburg, and was in operation between 1992 and 2007. It produced collisions between a beam of protons at energy $E_p = 920$ GeV and a beam of electrons or positrons at energy $E_e = 27.6$ GeV. The center of mass energy of the collision is $\sqrt{s} = 319$ GeV, and the maximal transfer momentum squared Q^2 is of the order 10^5 GeV^2 . The HERA collider has been constructed with an installation of four experimental halls, two were occupied by the H1 and ZEUS experiments which observe the collisions between beams and two were occupied by the fixed target experiments HERMES and HERAA-B.

1.2 DIS process at HERA

The Deep-Inelastic scattering (DIS) process plays an important role in the determination of proton structure and testing the validity of perturbative QCD. At HERA, the electron or positron interacts with the proton via an exchange of a virtual vector boson (off-shell particle). The final state is formed by a scattered lepton ($e^{+/-}, \nu_e$) and an hadronic final state X.

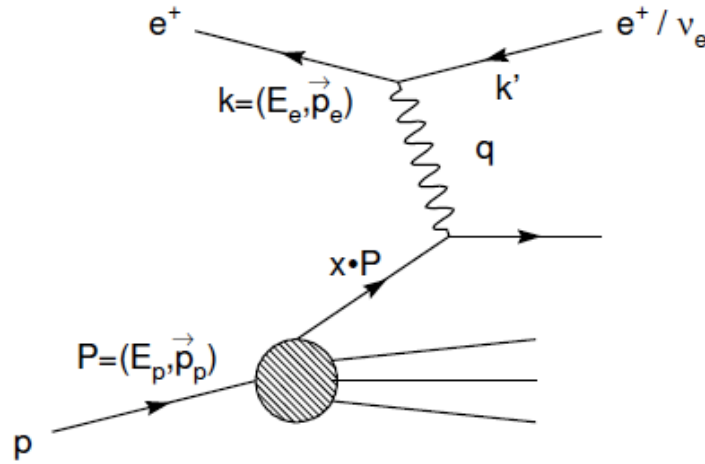


Fig. 1: Deep-inelastic process in lowest order

The nature of the exchanged vector boson classifies DIS into two types of interactions. Neutral current interaction (NC), if the interaction proceeds via the exchange of a photon or Z^0 and charged current interaction (CC), if the interaction proceeds via an exchange of a W^\pm . In the following we discuss the neutral current reaction which is at lowest order described by

the Feynman diagram shown in Fig. 1.

At a fixed center of mass energy $\sqrt{s} = \sqrt{(p_e + P)^2}$ the kinematics of the reaction is completely described by any two of the following variables: the four-momentum squared Q^2 , the Bjorken scaling variable x_{Bj} and the inelasticity variable y defined as

$$Q^2 = -q^2 = (p_e - p'_e)^2, \quad x_{Bj} = \frac{Q^2}{2P \cdot q}, \quad y = \frac{P \cdot q}{P \cdot p_e}. \quad (1)$$

where $p_e(p'_e)$ and P are the four-momentum of the initial (final) state lepton and proton, respectively.

In the present analysis, we want to measure the strong coupling constant α_s from H1 data. The Feynman diagram given in Fig. 1 does not contain an explicit strong vertex (the strong process is absorbed in the proton), so to measure α_s we have to use events with more than one parton in the final state.

1.3 Jet production in Deep-Inelastic Scattering

A jet is a set of hadrons, which deposits their energy into a region in the calorimeter, see Fig. 2, where several jets are suggested to the naked eye.

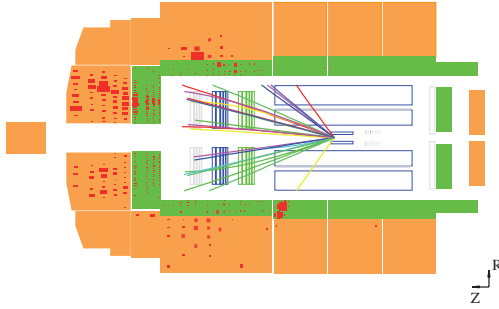


Fig. 2: DIS NC jet production event at H1

At leading order, 2-jet production (not counting the proton remnant jet) in DIS is described by the boson-gluon fusion and the QCD-Compton processes. Due to the first process, multi-jet cross section is sensitive to the gluon density in the proton. An example of a leading order contribution is given in Fig. 3.

At next-to-leading order, one has to consider the real and virtual contributions, of which a generic example is given in Fig3.

The variables characterizing the jet production are the invariant mass M_{ij} ,

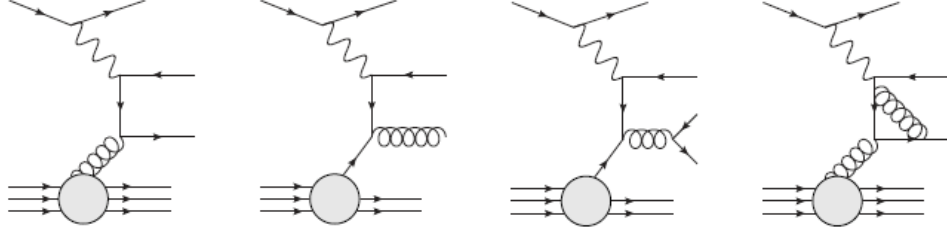


Fig. 3: Diagrams of different process in deep-inelastic lepton-proton scattering: Boson-gluon fusion process, QCD Compton process, Real NLO contribution and Virtual NLO contribution from right to left respectively

the partonic scaling variable x_p and the variable ξ defined by

$$\xi = x_{B_j} \left(1 + \frac{M_{ij}}{Q^2}\right) \quad x_p = \frac{x_{B_j}}{\xi} \quad (2)$$

The jet analysis is performed in the Breit frame where the virtual boson interacts head-on with the proton: $2x_{B_j}\vec{P} + \vec{q} = 0$, where \vec{P}, \vec{q} are the momentum of the proton and the virtual boson. Particles in the hadronic final state are clustered using the k_T algorithm. In this algorithm, pairs of particles are clustered in the order of increasing relative transverse momentum K between the particles.

2 Cross section calculation

2.1 NLO jet cross section

The DIS cross section is given by

$$\sigma = \sum_{m=1}^{\infty} \sum_a \int_0^1 dx f_a(x, \mu_f) \cdot \Gamma^{(m)}(\{p\}_m, x) |\mathcal{M}(\{p, a\})_m|^2 \cdot F_J(\{p\}_m), \quad (3)$$

where, m is the number of partons in the final state, a runs over all the flavors, x is the fraction of momentum of the parton of flavor a in the proton, f_a is the parton distribution function, $d\Gamma^m$, $\{p\}_m$ are the phase space and the set of momenta of the particles m respectively, \mathcal{M} is the matrix element of the partonic process and F_J is the jet function.

Considering only processes with n and $n+1$ partons in the final state. At next-to-leading order, the square matrix elements are approximated as

$$|\mathcal{M}(\{p, a\}_n)|^2 \simeq |\mathcal{M}^0(\{p, a\}_n)|^2 + \frac{\alpha_s}{2\pi} \cdot \mathcal{R}[\mathcal{M}^0(\{p, a\}_n) \cdot \mathcal{M}^1(\{p, a\}_n)] \quad (4)$$

and

$$|\mathcal{M}(\{p, a\}_{n+1})|^2 \simeq |\mathcal{M}^0(\{p, a\}_{n+1})|^2. \quad (5)$$

On the right hand side of eq (4), the first term correspond to the Born contribution, the second term corresponds to the virtual contribution (interference of the LO Feynman diagrams with the loop correction diagrams). The equation (5) corresponds to the real correction. In general, we can write the NLO cross section as

$$\sigma_{n-jet} = \sigma_{n-jet}^{LO} + \sigma_{n-jet}^{NLO} = \sigma_{n-jet}^{LO} + \left[\int_{n+1} d\sigma^R + \int d\sigma^V \right] \quad (6)$$

During the NLO calculation, three types of divergences appear. An ultraviolet divergence appear in the virtual contribution. This divergence is taken care of by renormalization procedure. Soft and collinear divergences appear in the real and virtual contributions. The first one is compensated between real and virtual contributions and the second one is absorbed in the parton distribution function.

The complex structure of these singularities make the analytical integration in the phase space very difficult. One can use the numerical integration, which requires the subtraction of these divergences to make the integral finite using the subtraction method [?].

2.2 fastNLO

”fastNLO” [3] provides a flexible method for a very fast numerical evaluation of an arbitrary cross section at next-to-leading order, and thus provides a quick method for fitting α_s and the PDFs.

2.2.1 fastNLO principle

Consider the following definition of the the DIS cross section

$$\sigma = \sum_{a,n} \int_0^1 dx c_{a,n} \left(\frac{x_{Bj}}{x}, \mu_r, \mu_f \right) \cdot [\alpha_s^n(\mu_r) \cdot f_{a/h}(x, \mu_f)]. \quad (7)$$

The basic idea of fastNLO is to rewrite the equation (7) into a factorizable expression where the convolution of the perturbative coefficient and the partonic density functions is reduced to a product.

In equation (7) the x -dependence of the PDFs and the factorization scale ($\mu_{r,f} = \mu$) in the PDFs and the strong coupling constant can be approximated using the following interpolation

$$\alpha_s^n(\mu) \cdot f_{a/h}(x, \mu) \simeq \sum_{k,l} \alpha_s^n(\mu^{(l)}) \cdot f_{a/h}(x^{(k)}, \mu^{(l)}) \cdot e^{(k)}(x) \cdot b^{(l)}(\mu), \quad (8)$$

where, $e(x), b(\mu)$ are the interpolation functions for the x and μ dependence respectively. Inserting (8) in (7)

$$\sigma = \sum_{a,n,l,k} \tilde{\sigma}_{n,a,k,l} \cdot \alpha_s^n(\mu^{(l)}) f_{a/h}(x^{(k)}, \mu^{(l)}), \quad (9)$$

where

$$\tilde{\sigma}_{n,a,k,l} = c_{n,a}(x, \mu) \cdot [e^{(k)}(x) \cdot b^{(l)}(\mu)]. \quad (10)$$

In equation (9), the cross section is given as a sum of a product where the PDFs are separated from the integration. The time consuming step of the procedure is only the computation of the $\tilde{\sigma}$ in (10) which involves integration over the phase space. This is done once, all further calculations to obtain the final cross section can be performed very fast and it will be easy to calculate the cross section for any arbitrary α_s and any arbitrary PDFs.

2.2.2 FastNLO Calculation

The fastNLO concept provides computer code and tables of pre-computed perturbative coefficients, which allows very fast computation of the jet cross sections for arbitrary PDFs and $\alpha_s(M_z)$. Tables and corresponding user-code are available on the fastNLO web site [4] for a large number of data-sets.

- Tables: The fastNLO calculations are based on tables of pre-computed perturbative coefficients, generated by NLOjet++ [5],[6]¹. These tables are available from the fastNLO web site.
- Specific code (or scenarios): The elementary pieces in fastNLO are called "scenarios". One scenario includes everything that is needed to compute the theory predictions for one measurement, usually corresponding to the results of one experimental publication.

In the present work, we use the fnh2003 table, which is generated by NLOjet++ version 1.4, where the number of events is 10 billions in LO and 37.82 blions in NLO. The renormalization and the factorization scales are chosen to be proportional to $\mu_0 = E_T$ (The E_T of jets). The double differential cross section $d^2\sigma_{jet}/dQ^2 dE_T$ for the 24 bins of Q^2 and E_T , as measured by the H1 collaboration[9], are calculated by fastNLO using CTEQ65 PDFs for a given value of $\alpha_s(M_z)$ ($\alpha_s(M_z) = 0.118$).

3 Fitting techniques

The fit of α_s is performed in a χ^2 minimization using the program minuit [7], where the definition of χ^2 takes into account all correlations of experimental and theoretical uncertainties.

¹ NLOjet++ is a program which calculates jet cross sections in next-to-leading order using the Monte Carlo technique

3.1 χ^2 definition

In our work we will consider the following definition of the χ^2 [8]

$$\chi^2(\alpha_s, \vec{\epsilon}) = \sum_i \frac{(\sigma_i^{exp} - \sigma_i^{the}(\alpha_s)[1 - \sum_k \delta_{i,k}(\epsilon_k)])^2}{\delta_{i,uncorr}^2} + \sum_k \epsilon_k^2, \quad (11)$$

where, the index i runs over the 24 measured cross section bins, σ_i^{exp} is the experimental cross section, $\sigma_i^{the}(\alpha_s) = \sigma_i^{fastNLO}(\alpha_s) \otimes [Z^0/hcor]$ calculated from fastNLO and taking into account the Z^0 and the hadronization corrections, k runs over all sources of correlated errors, $\delta_{i,k}$ is the contribution from k th correlated source to the i -th measurement, $\delta_{i,uncorr}$ is the uncorrelated uncertainty including the statistical uncertainty, the gaussian random variable ϵ_k correspond to the correlated errors and are allowed to be free in the fit parameters (see next section).

3.2 Source of errors

The following systematic uncertainties are considered

- Source of correlated errors:
 - Positron energy scale uncertainty
 - Positron polar angle uncertainty
 - Model dependence of the data correction
 - HFS scale uncertainty
 - Luminosity measurement uncertainty
 - QED radiative correction uncertainty
- Source of uncorrelated errors:
 - Statistical uncertainty
 - Model dependence of the data correction
 - positron energy uncertainty
 - positron polar angle uncertainty
 - HFS energy scale uncertainty

The dominant experimental uncertainties arise from the model dependence of the data correction and from the hadronic final state (HFS) energy scale uncertainty. The first five correlated uncertainties correspond to $\epsilon_1, \epsilon_2, \epsilon_3, \epsilon_4$ and ϵ_5 respectively in the definition of the χ^2 eq (11).

3.3 Minimization of χ^2 using Minuit

Minuit is a collection of minimization libraries developed at CERN by Fred James (1975). It is used to find the minimum value of a multi-parameter function and analyze the shape of the function around the minimum.

The basic concept of minuit is that it acts on a multi-parameter Fortran function called FCN, which calculates the χ^2 between the prediction and the data. In the present work, the parameters of FCN (or the parameters of the fit) are the α_s and ϵ_k .

The Minuit commands (Migrad, Minos and Hesse) request Minuit to minimize FCN with respect to the parameters, which correspond to the lowest value of χ^2 .

One can call Minuit in two modes, the "data-driven mode" and "Fortran callable mode". In our analysis, we use the first mode which contains three parts

- The User's FCN: It is a Fortran subroutine, calculates the theoretical cross section using fastNLO and calculates χ^2 which includes the fit parameters.
- The user's data to drive Minuit: where we give to the fit parameters the starting values and errors, fix or let one parameter or more free and call minuit commands.
- The User's main program: where we call Minuit.

4 α_s extraction

This section is dedicated to the principal subject of this work, which is the precise measurement of the strong coupling constant $\alpha_s(\mu_r)$. The value of the strong coupling constant is a function of the renormalization scale μ_r . Since this dependence is predicted by perturbative QCD, the value at any scale can be calculated from the value at a specific scale which usually chosen to be the Z_0 boson mass $M_z = 91.137\text{GeV}$ using the exact numerical solution of the renormalisation group equation.

The perturbative QCD prediction of the inclusive jet production cross sections are calculated in the \overline{MS} scheme using the fastNLO package, where the renormalization scale μ_r is identified with the transverse jet energy E_T . The analysis is performed in Breit frame, and the particles are clustered using the k_T algorithm. The cross section is determined using the CTEQ6.5 proton PDFs, assuming that the parton distributions are well known from independent measurement. Measurements and predictions are used to calculate the χ^2 with the Migrad, Minos and Hessian methods, where the parameters of the fit are chosen to be free with the starting value $\alpha_s = 0.118$ and $\epsilon_k = 0$ ($k = 1, \dots, 5$). The central value of $\alpha_s(M_z)$ is obtained from a fit of the double differential inclusive jet cross section $d^2\sigma_{jet}/dE_T dQ^2$, shown in Fig. 4, calculated by fastNLO and using the data collected in the year

1995-1997 corresponding to H1 collaboration publication in 2007 [9].

The results of the individual fitted values of $\alpha_s(E_T)$ are presented in the Fig. 5, and the common fit to α_s of all the 24 measurements yields:

$$\chi^2 = 20.275$$

$$\alpha_s(M_z) = 0.11781 \pm 0.00232$$

$$\epsilon_1 = -0.33 \pm 0.67$$

$$\epsilon_2 = 1.02 \pm 0.824$$

$$\epsilon_3 = 0.31 \pm 0.97$$

$$\epsilon_4 = 0.23 \pm 0.73$$

$$\epsilon_5 = 0.07 \pm 0.99$$

where we considered just the experimental errors.

Summary

I have successfully used the fastNLO program to calculate the NLO jet cross sections in DIS, and I have developed a method of fitting using Minuit. I applied this method to the α_s fit using H1 data collected in the years 1999 and 2000 and got a very precise results of $\alpha_s(M_z)$ which is in agreement with the H1 publication [9].

Also during my work in H1 group I learned how to use NLOjet++ to calculate NLO jet cross sections and the h1 fitter program package to fit PDFs and $\alpha_s(M_z)$.

References

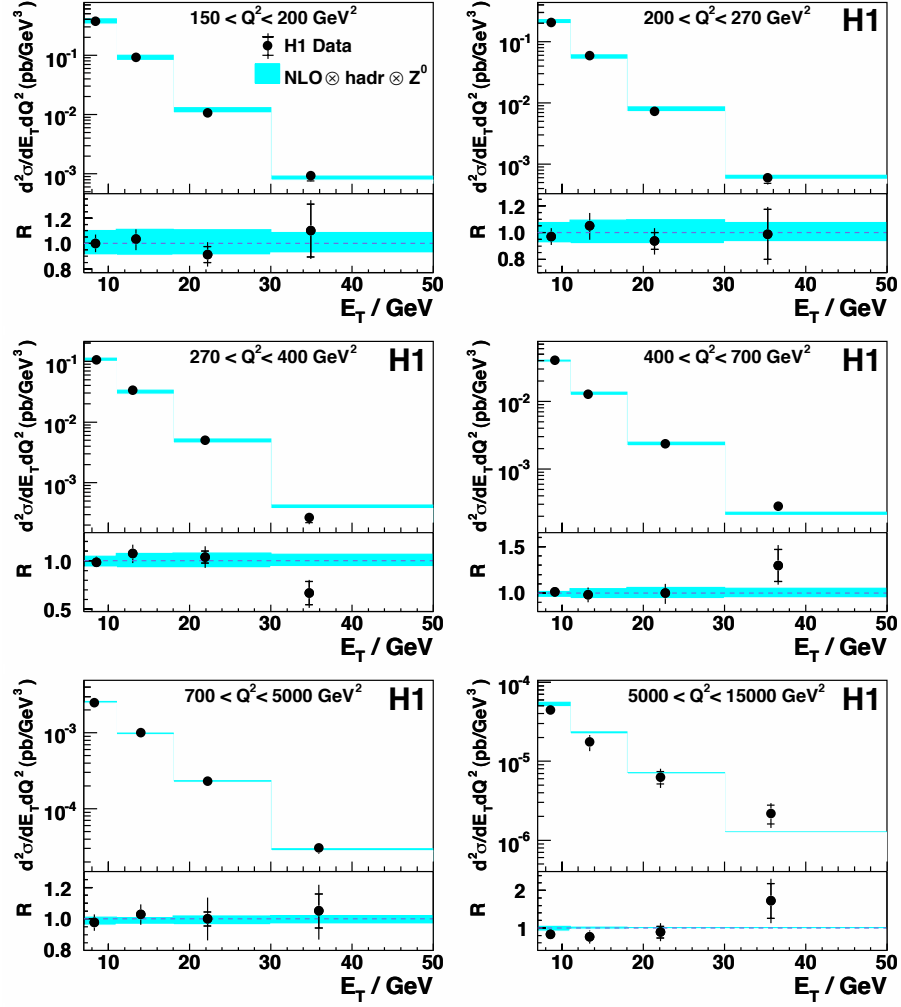
- [1] S. Catani, M.H. Seymour, A General Algorithm for Calculating, hep-ph/9605323 Jet Cross Sections in NLO QCD,
- [2] S. Catani, Yuri L. Dokshitzer, M. H. Seymour, and B. R. Webber. Longitudinally invariant Kt clustering algorithms for hadron hadron collisions. Nucl. Phys., B406:187224, 1993
- [3] T. Kluge, K. Rabbertz, M. Wobisch, fastNLO: Fast pQCD Calculations for PDF Fits, hep-ph/0609285 206.
- [4] <http://projects.hepforge.org/fastnlo/>
- [5] Z. Nagy, Phys. Rev. Lett. 88, 122003 (2002),
- [6] Z. Nagy, Phys. Rev. D68, 094002 (2003)
- [7] <http://wwwasdoc.web.cern.ch/wwwasdoc/minuit/minmain.html>
- [8] Markus Wobisch, PhD Thesis, RWTH Aachen (2000)PITHA 00/12
- [9] H1 Collaboration, DESY 07-073
- [10] H1 Collaboration, DESY 00-145
- [11] M. Gouzevitch, DESY-THESIS-2008-047

Thanks:

I would like to thank my supervisors Dr. Guenter Grindhammer and Daniel Britzger for trusting me and giving me the opportunity to work in this subject.

I want to thank Prof. Dr. Joachim Meyer and Andrea Schrader , for organizing DESY summer school program and making my stay at DESY very happy .

Inclusive Jet Cross Section



(a)

Fig. 4: The double differential cross section for inclusive jet production as a function of E_T for six regions of Q^2

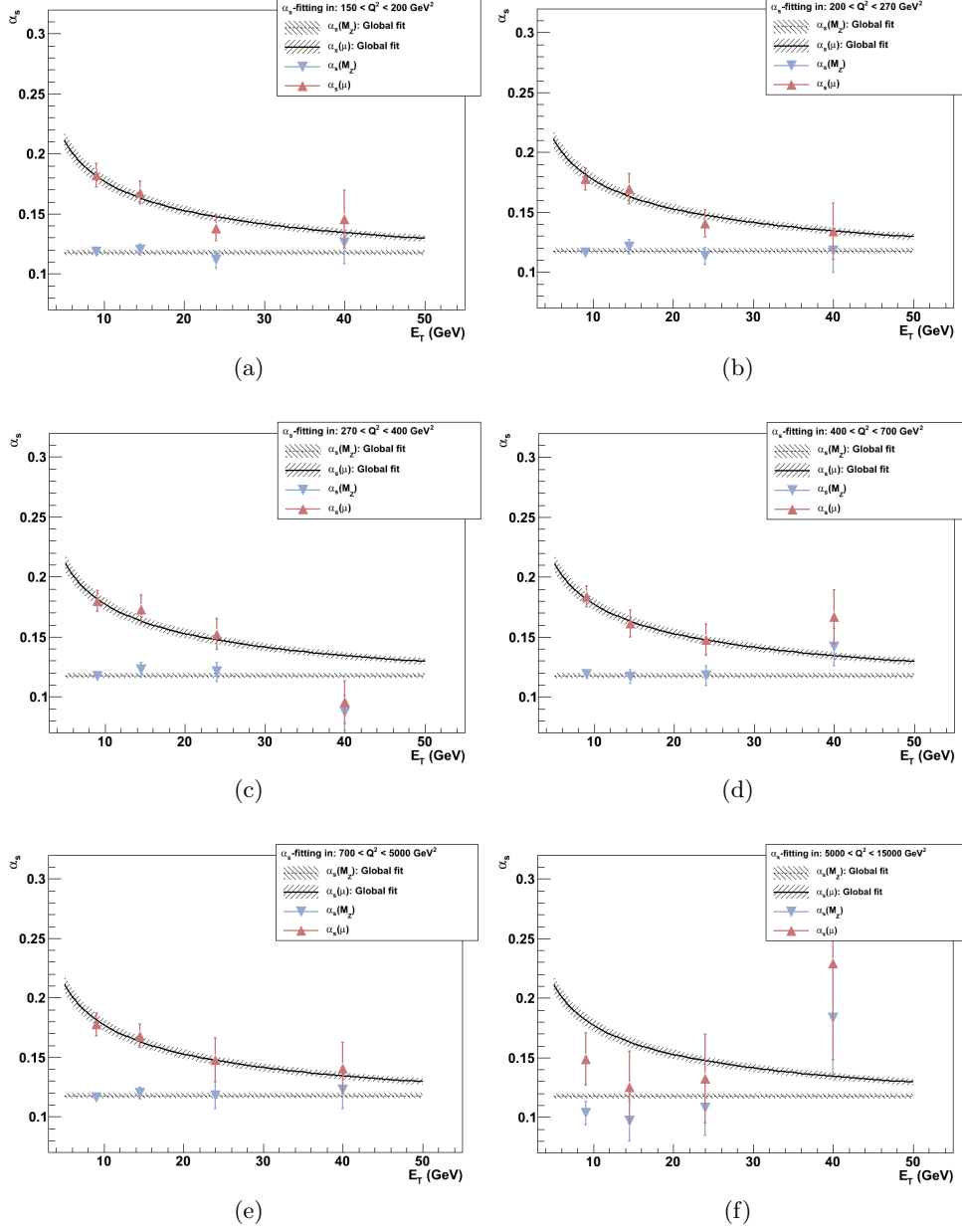


Fig. 5: Results of the fitted value of $\alpha_s(E_T)$ using the inclusive jet cross section for six regions of Q^2 . The solid line shows the two loop solution of the renormalization group equation evolving the averaged $\alpha_s(M_Z)$ from all determinations.